Lentinan induces apoptosis of mouse hepatocellular carcinoma cells through the EGR1/PTEN/AKT signaling axis

JINGPING YOU[1*], QICI WU[1*], YUNBING LI[1], XIUMIN LI[1,2], ZHICHAO LIN[1,3], JIAFU HUANG[1,3], YU XUE[1,3], ALITONGBIEKE GULIMIRAN[1,2] and YUTIAN PAN[1-3]

[1]Engineering Technological Center of Mushroom Industry, Minnan Normal University; [2]Fujian Universities Engineering Research Center of Fungus Industry, Minnan Normal University; [3]Fujian Engineering Technology Research Center of Fungal Active Substances, Zhangzhou, Fujian 363000, P.R. China

Received December 8, 2022; Accepted April 21, 2023

DOI: 10.3892/or.2023.8579

Abstract. Lentinan (LNT) isolated from *Lentinus edodes* is a vital host defense potentiator previously utilized as an adjuvant in cancer therapy. The present study investigated the effect of LNT on the mouse hepatocellular carcinoma (HCC) cell line Hepa1-6 and its possible mechanism. Mouse HCC apoptosis and its potential associated mechanism were then explored using *in vitro* and *in vivo* approaches. For *in vitro* approaches, the effect of LNT on the proliferation of Hepa1-6 cells was investigated by Cell Counting Kit-8 assay. Annexin V-FITC staining and flow cytometry were applied to explore HCC apoptosis. Western blotting was used to analyze related proteins, such as EGR1, phosphatase and tensin homolog (PTEN), phosphorylated protein kinase B (p-Akt), protein kinase B (Akt), B lymphocyte-2 (Bcl-2), Bcl2 family-associated X protein (Bax), etc. Cellular immunofluorescence staining was employed to assess the localization and expression of EGR1 and PTEN in nuclear and cytoplasmic fractions of Hepa1-6 cells. The association between *EGR1* and *PTEN* was explored by *EGR1* overexpression in cell lines. For *in vivo* methods, a mouse model of diethylnitrosamine (DEN)-induced primary liver cancer was established using C57BL/6 mice to investigate the inhibitory effect of LNT on liver cancer. Histopathology of liver tissue from mice was detected by hematoxylin-eosin staining and immunohistochemical assay. *In vitro* and *in vivo* results showed that LNT can inhibit the proliferation and promote the apoptosis of mouse HCC cells. Besides, LNT increased the expression of EGR1 in Hepa1-6 cells, which is translocated to the nucleus to function as a transcriptional factor. EGR1 then activates the expression of the tumor suppressor PTEN, thereby inhibiting the activation of the AKT signaling pathway. These data revealed a novel anti-tumor mechanism by which LNT can induce apoptosis to inhibit mouse HCC progression through the EGR1/PTEN/AKT axis. These results provide a scientific basis for the potential use of LNT in drug development and clinical applications associated with primary liver cancer.

Correspondence to: Dr Qici Wu or Professor Yutian Pan, Engineering Technological Center of Mushroom Industry, Minnan Normal University, 36 Xianqianzhi Road, Zhangzhou, Fujian 363000, P.R. China
E-mail: wuqiyang168@163.com
E-mail: pyt1106@mnnu.edu.cn

[*]Contributed equally

Abbreviations: LNT, lentinan; HCC, hepatocellular carcinoma; EGR1, early growth response-1; DEN, diethylnitrosamine; IF, immunofluorescence; IHC, immunohistochemical; PCNA, proliferation cell nuclear antigen

Key words: LNT, early growth response 1, PTEN, AKT, apoptosis

Introduction

Over the past decades, polysaccharides isolated from naturally-occurring sources, such as fungi, plants, and algae, are gradually recognized for their anti-tumor activity (1). In particular, these polysaccharides have been previously shown to significantly prolong the survival of patients with cancer whilst improving their quality of life when used as cancer therapeutics (2,3). Therefore, polysaccharides are potential candidates for cancer therapy. Lentinan (LNT) is a polysaccharide that can be isolated from the mushroom species *Lentinus edodes*. It has various reported biologically active properties, including immunomodulatory, anti-tumor, antiviral and antibacterial effects, in addition to high efficacy and minimal side effects (4). As the first medicinal macrofungal polysaccharide drug to enter the field of modern biotechnology (5), its unique triple-helix conformation and antitumor activity have particularly attracted attention (6). Several studies have shown that LNT can mediate anti-tumor effects directly and indirectly (7-10). A previous study found that LNT can exert inhibitory effects in a mammary-specific polyomavirus middle T antigen overexpression mouse model of spontaneous breast cancer (7). However, the anti-tumor mechanism of LNT remains to be fully elucidated, where the relevant signaling pathways involved remains poorly understood. In the majority of cases, it is used as an adjuvant therapeutic agent in clinical practice, potentially limiting global application.

According to data from a 2020 Global Cancer Report published by the International Agency for Research on Cancer of the World Health Organization, liver cancer has the sixth highest incidence and third highest mortality rate of all cancers worldwide (11). Despite the progress made regarding its diagnosis and treatment methodologies, both morbidity and mortality rates from liver cancer continue to rise (11). Identification of effective methods for preventing and treating liver cancer remains in urgent demand. From the perspective of hepatocarcinogenesis, changes in transcription factor expression, dysregulated signaling pathways, and alterations in the tumor microenvironment are all considered to be factors that can promote this process (12,13). If these factors can be restored to their pre-cancerous state, then the malignant behavior of the tumor can be inhibited (14).

Recently, bioinformatics approaches have been used to screen for genes that are abnormally expressed in primary liver cancer (15,16). Among these aberrant genes, *early growth response 1* (*EGR1*) was found to be a potential target for developing drugs against primary liver cancer (16). *EGR1* belongs to the EGR protein family member. The *EGR1* gene is located in human chromosome region 5q23-31, where the corresponding EGR1 protein is an important transcription factor and belongs to the EGR protein family member (17). It has been reported that EGR1 is a transcription factor of the PTEN tumor suppressor gene, which also transactivates p53, p73, p300/CBP, and other pro-apoptotic and anti-oncogenes (18).

In the present study, the mechanisms by which LNT can inhibit liver cancer physiology were investigated using both *in vitro* and *in vivo* experimental methods. Various cellular and molecular techniques *in vitro* were applied to study the relationship between the impact of LNT on mouse hepatocellular carcinoma (HCC) cell line Hepa1-6 and the abnormal expression of EGR1 in HCC cells. Then the mouse model of diethylnitrosamine (DEN)-induced primary liver cancer was used for further verification *in vivo*. These results provide a scientific basis for the future development and clinical application of LNT as a treatment for primary liver cancer.

Materials and methods

Cell culture and treatment. The mouse HCC cell line Hepa1-6 was purchased from The Cell Bank of Type Culture Collection of the Chinese Academy of Sciences. Cells were cultured in RPMI-1640 medium (cat. no. MA0215; Dalian Meilun Biology Technology Co., Ltd.) supplemented with 10% FBS (cat. no. 164210-50; Procell Life Science & Technology Co., Ltd.) and 1% penicillin-streptomycin at 37˚C in a 5%-CO_2 incubator.

Cells were treated with a series of LNT dosages (0, 250, 500 and 1,000 μg/ml) for 24 h. LNT was prepared from *Lentinus edodes* by the Engineering Technological Center of Mushroom Industry and confirmed to be essentially consistent with standards obtained from Jinling Pharmaceutical Co., Ltd. (Nanjing, China).

Cell viability assay. Cellular growth and proliferation in different groups were monitored via optical microscope and detected with Cell Counting Kit-8 (CCK-8; cat. no. A311; Vazyme Biotech Co., Ltd.) according to the manufacturer's protocol. Briefly, Hepa1-6 cells in the logarithmic growth phase were inoculated into a 96-well microplates at a density of $2x10^3$ cells per well at 37˚C for 12 h. After the cells adhered to the plate wall, the supernatant was discarded and the cells were treated with different concentrations of LNT (0, 250, 500 and 1,000 μg/ml) in a humidified atmosphere containing 5% CO_2 for 12 and 24 h, respectively. Then, 10 μl of CCK-8 reagent was added into each well and incubated for 2 h at 37˚C. The absorbance at 450 nm was measured using a microplate reader (Infinite M200 PRO; Tecan Group, Ltd.). Cell viability was calculated as follows: Cell viability (%)=(As-Ab)/(Ac-Ab) x100%, where Ab, As, and Ac were the values of the blank medium, experimental group, and control group, respectively.

Apoptosis staining. Hepa1-6 cells ($6x10^4$) were inoculated into six-well plates, and cultured until adherence, before being treated with different dosages of LNT for 24 h at 37˚C. Next, *in situ* fluorescence staining was performed using an Annexin V-FITC Apoptosis Detection kit (cat. no. C1062L; Beyotime Institute of Biotechnology). Fluorescence was observed under a fluorescence microscope (BX51; Olympus Corporation). FITC and propidium iodide (PI) staining were associated with green and red fluorescence, respectively.

Flow cytometry. Hepa1-6 cells were inoculated and treated with LNT according to the method that was performed for the apoptosis assay. As a positive control, cells were also treated for 24 h at 37˚C with a mixture of 100 μmol/l $FeSO_4$ and 500 μmol/l H_2O_2. FITC and PI staining were performed using an Annexin V-FITC Apoptosis Detection kit. Fluorescence was measured by flow cytometry (Flowsight; Merck KGaA) and apoptosis was analyzed for each group of cells using the FlowSight software.

Western blotting (WB). For samples in each group, total protein was extracted from cells or tissues by WB and IP cell lysates (cat. no. P0013; Beyotime Institute of Biotechnology) before the BCA Protein Assay kit (cat. no. 23227; Thermo Fisher Scientific, Inc.) was used for quantification. Protein samples (20 μg per well) were subjected to SDS-PAGE on an 8% gel, transferred onto PVDF membranes (cat. no. 3010040001; Roche Diagnostics) after electrophoresis and blocked with NcmBlot blocking buffer (cat. no. P30500; New Cell & Molecular Biotech) for 20 min at room temperature. The membranes were then incubated with primary antibodies (1:1,000) overnight at 4˚C, before being incubated with HRP-conjugated anti-rabbit or anti-mouse secondary antibodies for 1 h at room temperature. Finally, an ECL luminescent solution (cat. no. MA0186-1; Dalian Meilun Biology Technology Co., Ltd.) was added and the target protein was detected by exposure using an Omega Lum C Gel Imaging system (Gel Company, Inc.). Quantitative protein analysis was performed using ImageJ software (version: 2.1.0/1.53c; National Institutes of Health).

The following primary antibodies were used: Rabbit EGR1 (cat. no. 55117-1-AP; ProteinTech Group, Inc.), rabbit PTEN (cat. no. AF6351), rabbit phosphorylated (p)-AKT (cat. no. AF0016), rabbit AKT (cat. no. AF6261), mouse Bcl-2 (cat. no. BF9103), rabbit Bax (cat. no. AF0120), rabbit poly (ADP ribose) polymerase 1 (PARP1; cat. no. 13371-1-AP), rabbit heat shock protein 60 (Hsp60; cat. no. AF0184), rabbit

proliferating cell nuclear antigen (PCNA; cat. no. AF0239) and mouse β-actin (cat. no. T0022; all from Affinity Biosciences).

The following secondary antibodies were used: Goat anti-Mouse IgG (H + L) Cross-Adsorbed Secondary Antibody, Alexa Fluor™ 488 (cat. no. A-11001), and Goat anti-Rabbit IgG (H+L) Cross-Adsorbed Secondary Antibody, Alexa Fluor™ 488 (cat no. A-11008; both from Thermo Fisher Scientific, Inc.).

Overexpression of EGR1 in cell lines. To induce the overexpression of *EGR1*, according to the mouse *EGR1* mRNA sequence on NCBI (NM-007913.5), the specific primers were designed by Primer Premier 5.0 software (Premier Biosoft International), and 15 bp eukaryotic expression plasmid pCMV-Myc (cat no. 11910ES03; Shanghai Yeasen Biotechnology Co., Ltd.) homologous sequence was added at both ends (Table I). Total RNA was extracted from Hepa1-6 cells by TRIzol Universal (cat. no. DP424; Tiangen Biotech Co., Ltd.) and reverse transcribed into cDNA by PrimeScript™ RT reagent kit (Perfect Real Time) (cat. no. RR037 A; Takara Biotechnology Co., Ltd.). Using this as a template, PCR was carried out with primers (cat. no. 10154; Shanghai Yeasen Biotechnology Co., Ltd.). The reaction procedure is shown in Table II. PCR products were isolated by 1% agarose gel with YeaRed Nucleic Acid Gel Stain (10,000X in DMSO) (cat. no. 10202ES30; Shanghai Yeasen Biotechnology Co., Ltd.) and separated from the gel with a DNA extraction kit (cat no. B518131; Sangon Biotech Co., Ltd.). Subsequently, the pEASY®-Basic Seamless Cloning and Assembly Kit (cat. no. CU201-02; Beijing Transgene Biotech Co., Ltd.) was applied to clone the amplified cDNA into the linear pCMV-Myc plasmid fragment recovered by *Eco*RI restriction enzymes (cat. no. R0101; New England Biolabs). The correctly sequenced strains were amplified, and the plasmids were extracted with TIANprep Mini Plasmid kit (cat. no. DP106; Tiangen Biotech Co., Ltd.) for subsequent cell transfection.

Cell transfection. Hepa1-6 cells ($5x10^5$) were seeded into a six-well plate and cultured in 500 μl serum- and antibiotics-free medium. When the cell density reached about 90%, the cells were transfected with the plasmids. According to the protocol of Hieff Trans™ Liposomal Transfection Reagent (cat no. 40802ES03; Shanghai Yeasen Biotechnology Co., Ltd.), 4 μg of plasmid DNA and 10 μl of Hieff TransTM liposome nucleic acid transfection reagent was mixed with 250 μl of OPTI-MEMI medium and incubated at room temperature (25˚C) for 5 min, respectively. Subsequently, the diluted plasmid DNA and liposome nucleic acid transfection reagent were mixed evenly and incubated at room temperature (25˚C) for 20 min to form DNA- liposome complex. Then, 500 μl of DNA-liposome complex was added into each plate well and cultured at 37˚C in a 5%-CO_2 incubator for 24 h. When necessary, after transfection for 6 h, the cells were cultured with a complete medium for improved transfection activity. Finally, mediums containing gradient concentration of LNT (0, 250, 500, and 1,000 μg/ml) were applied to culture for another 24-h incubation. WB was used to detect the expression level of EGR1 protein.

Separation of nuclear and cytoplasmic fractions. After 24 h of treatment with gradient concentrations of LNT at 37˚C, nuclear and cytoplasmic proteins were extracted and separated using a Nuclear and Cytoplasmic Protein Extraction kit (cat. no. P0028; Beyotime Institute of Biotechnology). Finally, WB was used to detect the expression of EGR1 protein in the two intracellular compartments.

Table I. Primer sequences used for reverse transcription PCR.

Gene name	Primer sequence (5'→3')
mEGR1	F: CATGGAGGCCCCGAATTATGAGC GGCCAAGG
	R: CTGGTCGACCGAATTGCAATTTC AATTGTCCTGG
pCMV-myc	F: TCTAAAAAGCTGCGGAATTGT
	R: TCCAAACTCATCAATCAATGTATC

F, forward; R, reverse; EGR1, early growth response 1.

Table II. Thermocycling conditions of PCR.

Temperature (˚C)	Duration	Number of cycles
98	3 min	1
98	10 sec	35
68	30 sec	35
72	5 min	1
4	∞	

Immunofluorescence (IF) staining. Clean slides were placed into 24-well plates for cell spreading, with six replicate wells set up for each group. Cells at a density of $1x10^5$ cells per well were allowed to adhere before being treated with gradient concentrations of LNT for 24 h at 37˚C, after which they were fixed with 4% paraformaldehyde solution at room temperature for 15 min. Cells were then washed three times with PBS, penetrated with 0.5% Triton X-100 for 20 min, and blocked with donkey serum (cat. no. MB4516; Dalian Meilun Biology Technology Co., Ltd.) for 30 min at room temperature (25˚C). Subsequently, they were incubated with a mixture of different primary antibodies, including mouse EGR1 (1:100; cat. no. H00001958-M03; Novus Biologicals, LLC) and rabbit PTEN (1:100; cat. no. AF6351; Affinity Biosciences), overnight at 4˚C. The cells were then washed with PBS and incubated with fluorescently-labeled secondary antibody (1:200) for 1 h at room temperature (25˚C) in the dark. After staining nuclei with DAPI (1:5,000; cat. no. C1002; Beyotime Institute of Biotechnology) for 5 min at room temperature, cells were sealed with anti-fluorescence quenching sealing solution (cat. no. P0126; Beyotime Institute of Biotechnology). Finally, images were collected using a laser scanning confocal microscope (Leica TCS SP8; Leica Microsystems GmbH).

Secondary antibodies used in IF staining were as follows: Donkey anti-rabbit IgG (H + L) highly cross-adsorbed secondary antibody labeled with Alexa Fluor Plus 555 (cat. no. A32794) and donkey anti-mouse IgG (H + L) highly

cross-adsorbed secondary antibody labeled with Alexa Fluor 488 (cat. no. A-21202; both from Invitrogen; Thermo Fisher Scientific, Inc.).

Mouse model of DEN-induced primary liver cancer. All protocols involving animals in the present study were reviewed and approved (approval no. 2020010) by the Animal Ethics and Welfare Committee of Minnan Normal University (Zhangzhou, China). Mice were obtained from Jiangsu Huachuang Xinuo Pharmaceutical Technology (certificate no. 320928211100002573).

In total, 40 female mice (C57BL/6 background) with gestational ages of 11-12 days were housed in a temperature (25˚C) and humidity (50-60%)-controlled room, where they were kept on a 12-h light/dark cycle and received autoclaved water and food *ad libitum* under specific pathogen-free conditions. After the pregnant mice gave birth, 1-week-old mice were acclimatized and fed for 1 week, after which 2-week-old male offspring (weight, ~15 g) were selected. A total of 40 mg/kg DEN (cat. no. HY-N7434; MedChemExpress) was injected intraperitoneally. Following the establishment of the model, mice were randomly divided into the following four groups (8 mice/group): i) Model group; ii) LNT-low dosage group (0.865 mg/kg); iii) LNT-middle dosage group (1.73 mg/kg); and iv) LNT-high dosage group (3.46 mg/kg). Meanwhile, another 8 mice of the same batch without DEN induction were used as the normal group. Each group of mice was treated via intragastric administration for 8 weeks. The normal group and model group were given an equivalent amount of saline. In the late stage of the experiment, the mice in the control group began to present slow movement and hair loss. At the end of the administration, the mice were anesthetized by intraperitoneal injection of ketamine (100 mg/kg) and xylazine (10 mg/kg), and were sacrificed by cervical dislocation. When cessation of breath and heartbeat was observed, they were subjected to autopsy for observation.

Hematoxylin-eosin (H&E) staining. Mouse liver tissues were fixed in a 10% paraformaldehyde solution at 4˚C, embedded in paraffin, and sectioned into 5-μm sections. The sections were deparaffinized with xylene and hydrated with gradient ethanol. H&E staining was then performed according to standard techniques. The sections were incubated with a hematoxylin solution (cat no. ZLI-9610; Beijing Zhongshan Golden Bridge Biotechnology Co., Ltd.; OriGene Technologies, Inc.) for 2 min at room temperature (25˚C) and washed with water for 6 min. Then, the sections were soaked in 70% ethanol solution containing 1% hydrochloric acid for 30 sec at room temperature (25˚C) and washed with water for 6 min again. Subsequently, they were stained with eosin (cat no. ZLI-9613; Beijing Zhongshan Golden Bridge Biotechnology Co., Ltd.; OriGene Technologies, Inc.) for 4 min at room temperature (25˚C) and rinsed with water for 6 min. Finally, the stained sections were examined using an Olympus fluorescent inverted microscope (IX71; Olympus Corporation).

Immunohistochemical (IHC) assay. Tissue expression levels of EGR1 and PTEN proteins were assessed by IHC. Liver tissue sections were deparaffinized with xylene and hydrated with decreasing concentrations of ethanol, after which they were treated for antigen retrieval with 0.01 mM citric acid buffer in a microwave. Endogenous peroxidase activity was inhibited by endogenous hydrogen peroxide (3% H_2O_2) treatment. Sections were then blocked with goat serum (cat no. MB4508-1; Dalian Meilun Biology Technology Co., Ltd.) for 1 h at room temperature (25˚C) and incubated overnight at 4˚C with rabbit EGR1 (1:200), rabbit PTEN (1:200) or rabbit Ki-67 (1:200; cat. no. ab15580; Abcam). The sections were then treated by IHC kits (cat. no. PV-9001/PV-9002; Beijing Zhongshan Golden Bridge Biotechnology Co., Ltd.; OriGene Technologies, Inc.) following the manufacturer's protocol. Sections were stained with DAB and counterstained with hematoxylin. Finally, sections were dehydrated in increasing concentrations of ethanol and xylene before being observed and imaged using an Olympus IX71 inverted microscope.

Statistical analysis. All statistical analyses were performed using GraphPad Prism 8 (Dotmatics). All experiments were repeated independently in triplicate. Data are expressed as the mean ± standard error of the mean (SEM) and analyzed by the independent sample t-test (between two groups) or one-way ANOVA variance analysis with Tukey's multiple comparisons (among-group comparisons), respectively. $P<0.05$ was considered to indicate a statistically significant difference.

Results

Effect of LNT on apoptosis in mouse HCC cells. CCK-8 method was used to explore the effect of LNT on the proliferation of Hepa1-6 cells. As revealed in Fig. 1A, the effect of LNT on Hepa1-6 cell viability rate increased with the increasing concentration of LNT. The lower concentration of LNT had no apparent toxicity to cells. However, medium and high concentrations of LNT (500~1,000 μg/ml) had a specific inhibitory effect on Hepa1-6 cell viability rate. The Annexin V-FITC staining method was used to detect the apoptosis of Hepa1-6 cells *in situ*. Early-stage apoptotic cells were stained with green fluorescence (FITC) only, while late-stage apoptotic cells or necrotic cells were double-stained with green and red fluorescence (PI). However, healthy cells were not fluorescently stained. As demonstrated in Fig. 1B, after the Hepa1-6 cells were treated with increasing concentrations of LNT, the green fluorescence became correspondingly more intense. When the LNT concentration reached 1,000 μg/ml, the degree of early-stage apoptosis appeared the most severe. In addition, flow cytometric analysis demonstrated that the total apoptotic rate of Hepa1-6 cells increased gradually with the increase of LNT concentration, and the LNT treatment at 1,000 μg/ml was more significant. (Fig. 1C). Bcl-2 and Bax, two markers in the Bcl-2 gene family, are closely associated with apoptosis (19). Bcl-2 is considered a representative anti-apoptotic marker (20), whilst Bax is a pro-apoptotic marker in the Bcl-2 family (21,22). After treatment with LNT for 24 h, total protein was extracted from each group for detection using WB. With increasing LNT concentrations, expression of the anti-apoptotic protein Bcl-2 was decreased, whilst expression of the pro-apoptotic protein Bax was increased, resulting in a significant reduction in the Bcl-2/Bax ratio (Fig. 1D). This suggested that LNT could induce apoptosis in Hepa1-6 cells.

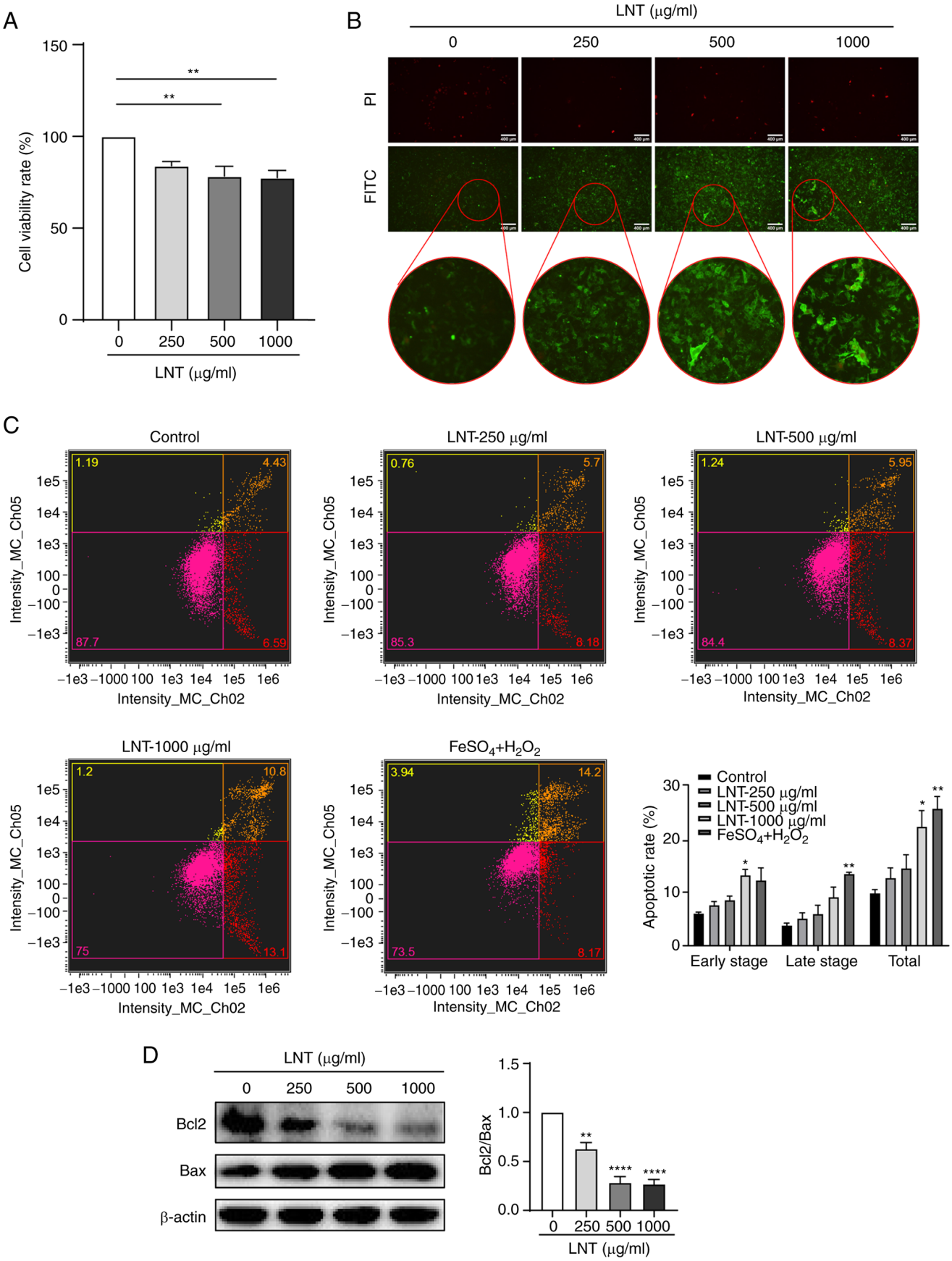

Figure 1. LNT-induced apoptosis of the mouse hepatocellular carcinoma cell line Hepa 1-6 *in vitro*. (A) Cell Counting Kit-8 assay was used to detect the effect of LNT on the proliferation of Hepa1-6 cells. (B) Apoptosis of Hepa1-6 cells treated with gradient concentrations of LNT as detected by the Annexin V-FITC Apoptosis Detection Kit. Fluorescence images were observed at x200 magnification. Scale bars, 400 μm (white). (C) Apoptosis was assessed by flow cytometry after LNT treatment. Cells treated with a mixture of $FeSO_4$ and H_2O_2 were used as a positive control. (D) Expression of the apoptotic markers Bcl-2 and Bax proteins as analyzed by western blotting. All data for related proteins were normalized using β-actin as the loading reference. *P<0.05, **P<0.01 and ****P<0.0001. LNT, Lentinan.

LNT induces apoptosis of Hepa1-6 cells through the EGR1/PTEN/AKT axis. A previous study has shown that inhibition of AKT phosphorylation in Hepa1-6 cells and mouse HCC models can cause changes in Bax expression, leading to apoptosis (23). Furthermore, increased expression of PTEN can inhibit AKT phosphorylation, thereby affecting downstream signaling pathways through apoptosis or cell cycle arrest, exerting a tumor suppressor function (24-28). EGR1 is considered a transcription factor of PTEN (29,30). Therefore, the present study next assessed whether LNT treatment can cause changes in the expression of EGR1, PTEN, and Akt phosphorylation in Hepa1-6 cells. From the WB data, it was found that the protein expression levels of EGR1 and PTEN were both significantly increased in Hepa1-6 cells with increasing LNT concentrations. By contrast, the level of Akt phosphorylation demonstrated the opposite trend, particularly p-Akt/Akt ratio decreased significantly (Fig. 2A).

Based on the upregulation of EGR1 expression after LNT treatment in Hepa1-6 cells, cell localization of EGR1 was, therefore, further explored under the same treatment conditions. By co-staining for EGR1 and PTEN with IF, the expression levels and cellular localization patterns of EGR1 and PTEN in Hepa1-6 cells treated with a gradient of LNT concentrations were assessed. These results showed that, in the control group, the weak fluorescence intensity of EGR1 (green) and PTEN (red) was indicative of a low expression level for EGR1 and PTEN. In the LNT-treated group, the fluorescence intensity of EGR1 (green) and PTEN (red) gradually increased, that is, the expression levels of EGR1 and PTEN gradually increased with the increase of LNT concentration, and the green fluorescence emitted by EGR1 was significantly enhanced in the nucleus after administration (Fig. 2B). A subsequent nuclear-cytoplasmic separation experiment revealed that with the increase of LNT concentration, EGR1 expression gradually increased in the nucleus and decreased in the cytoplasm, and the difference was significant (Fig. 2C). These results suggested that LNT could regulate both the expression and nuclear translocation of EGR1 in Hepa1-6 cells. After EGR1 enters the nucleus, it may function as a transcription factor to promote PTEN expression.

To further explore whether EGR1 is an upstream signaling molecule of PTEN and p-Akt, an *EGR1* overexpression system was constructed. EGR1, PTEN, p-Akt and Akt expression were all detected by WB. EGR1 overexpression was found to lead to significantly increased PTEN expression and p-Akt/Akt ratio decreased (Fig. 2D). These results suggested that EGR1 was the upstream signal of PTEN and Akt.

Taken together, it was identified that LNT treatment could restore EGR1 expression in mouse HCC cells and allow EGR1 to serve its normal function as a transcription factor, in turn promoting PTEN expression. This then inhibits the AKT signaling pathway, which alters the expression of downstream proteins Bcl-2 and Bax to ultimately trigger the apoptosis of mouse HCC cells.

DEN-induced primary liver cancer model in C57BL/6 mice. A primary liver cancer model was established using C57BL/6 mice induced by DEN, after which normal, model and three LNT administration groups were defined. Hyperplastic nodules could be observed on the liver surfaces of mice in the model group compared with those in the normal group. After treatment with LNT, the number of hyperplastic nodules on the liver was significantly reduced in the LNT-treated group compared with that in the model group (Fig. 3A and B). In addition, the tumor volume was significantly decreased (Fig. 3C). H&E staining was used to further observe the pathological situation of tumor tissue. The results revealed that in the model group, the tissue structure of the liver tumor changed significantly and fatty degeneration appeared in certain areas. The morphology and structure of the LNT-treated group were improved compared with the model group. The tumor area was relatively small, and the liver tissue structure in the high-dose group was close to the normal group (Fig. 3D).

In addition, WB and IHC staining were further applied to detect the difference of related protein expression. Changes in the expression of the relevant proteins between the normal and model groups are shown in Fig. 4A. Specifically, compared with the normal group, the model group exhibited significantly reduced expression levels of EGR1 and PTEN, whilst p-Akt/Akt ratio increased, indicating that Akt was activated significantly. The expression levels of proliferation-associated protein PCNA and the anti-apoptotic protein Bcl-2 were significantly increased, whilst those of the pro-apoptotic protein Bax were significantly decreased. The ratio of Bcl-2/Bax, an indicator of cell apoptosis, was significantly increased in the model group. These results suggested that compared with those in the normal liver tissue, there was no significant apoptosis in the liver cancer tissue of the model group, where the expression levels of EGR1 and PTEN were inhibited.

Using WB, it was also identified that compared with the model group the expression levels of EGR1 and PTEN were significantly increased in the LNT-treated group (Fig. 4B). In addition, the p-Akt/Akt ratio was significantly decreased, suggesting that AKT activity was inhibited. The expression levels of Bcl-2 and PCNA expression were significantly decreased, and Bax expression was increased, whilst Bcl-2/Bax ratio decreased. IHC analysis revealed that the protein Ki-67, which is associated with cancer cell proliferation, was markedly reduced with increasing LNT dosages in the LNT administration groups, compared with that in the model group. By contrast, the expression levels of EGR1 and PTEN were markedly increased, with EGR1 mainly distributing to the nucleus (Fig. 4C).

The results of these *in vivo* experiments are consistent with those found in the *in vitro* experiments. Therefore, it was considered that LNT could regulate EGR1 expression in mouse HCC cells, supporting its role as a transcription factor that can promote the expression of PTEN. PTEN then inhibits the PI3K/AKT signaling pathway and alters the expression of related apoptotic proteins Bcl-2 and Bax, ultimately inducing apoptosis and inhibiting the development of HCC.

Discussion

Over the past decade, the focus of cancer therapeutics has shifted from anti-proliferative effects to the development of agents that can induce cancer cell differentiation and apoptosis (31). Correspondingly, apoptosis-inducing drugs must selectively target cancer cells whilst protecting normal cells from apoptosis. Naturally-occurring compounds are

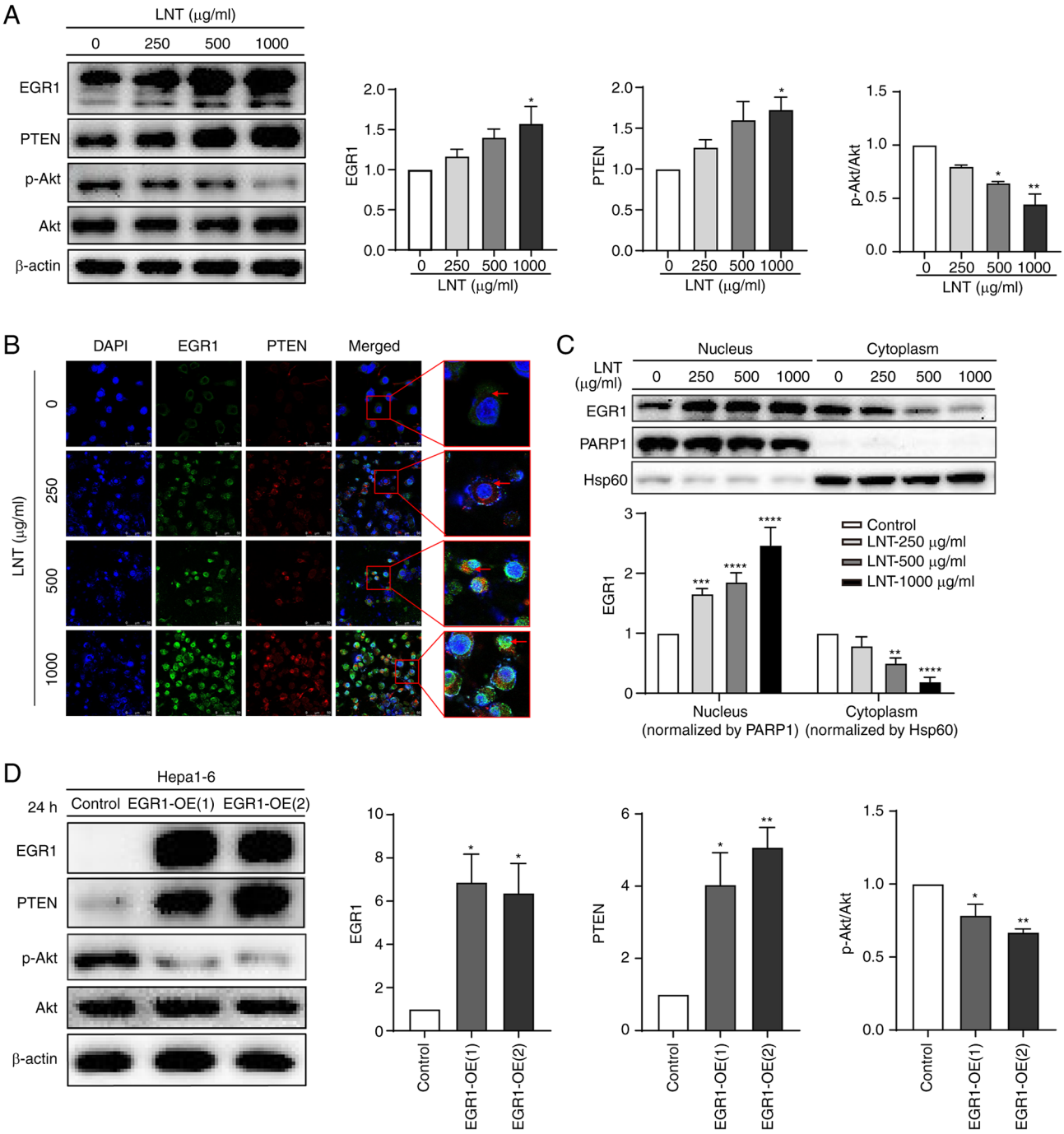

Figure 2. Effects of LNT on the EGR1/PTEN/AKT axis in Hepa1-6 cells. (A) Protein expression levels of EGR1, PTEN, p-Akt and phosphorylation of Akt after treatment with a gradient of LNT concentrations as detected by WB. All data for protein expression were normalized using β-actin as a loading reference. (B) Immunofluorescence co-staining was used to assess the localization and expression of EGR1 and PTEN in Hepa1-6 cells treated with a gradient of LNT concentrations. Images were observed at x630 magnification. Scale bars, 50 μm (white). (C) WB was used to detect the expression of EGR1 in the nuclear and cytoplasmic fractions following treatment with a gradient of LNT concentrations. (D) WB was used to detect the expression of EGR1, PTEN, p-Akt, and phosphorylation of Akt after *EGR1* overexpression. *P<0.05, **P<0.01, ***P<0.001 and ****P<0.0001. LNT, Lentinan; EGR1, early growth response 1; p-, phosphorylated; PARP1, poly-(ADP ribose) polymerase 1; Hsp60, heat shock protein 60; OE, overexpression; WB, western blotting.

characterized by low toxicity, providing them the potential to greatly improve the patient quality of life following treatment (32). Therefore, it is of particular importance to identify natural compounds that can selectively inhibit the initiation, development and metastasis of cancer cells whilst eliminating cancer stem cells, without toxic effects on normal cells (32). LNT was firstly discovered and extracted by Chihara *et al* from the fruiting body of *Lentinula edodes* (33,34). It is a bioactive polysaccharide currently used as an adjuvant therapy for cancer and other diseases (35-37). Although it has been suggested that LNT is not directly toxic to cancer cells (38,39), the present experimental results demonstrated that LNT could induce apoptosis in mouse HCC cell line Hepa1-6 cells *in vitro*. Previous studies have also reported that LNT can directly induce cancer cell apoptosis in colon cancer (40), cervical cancer (41) and lung adenocarcinoma (42).

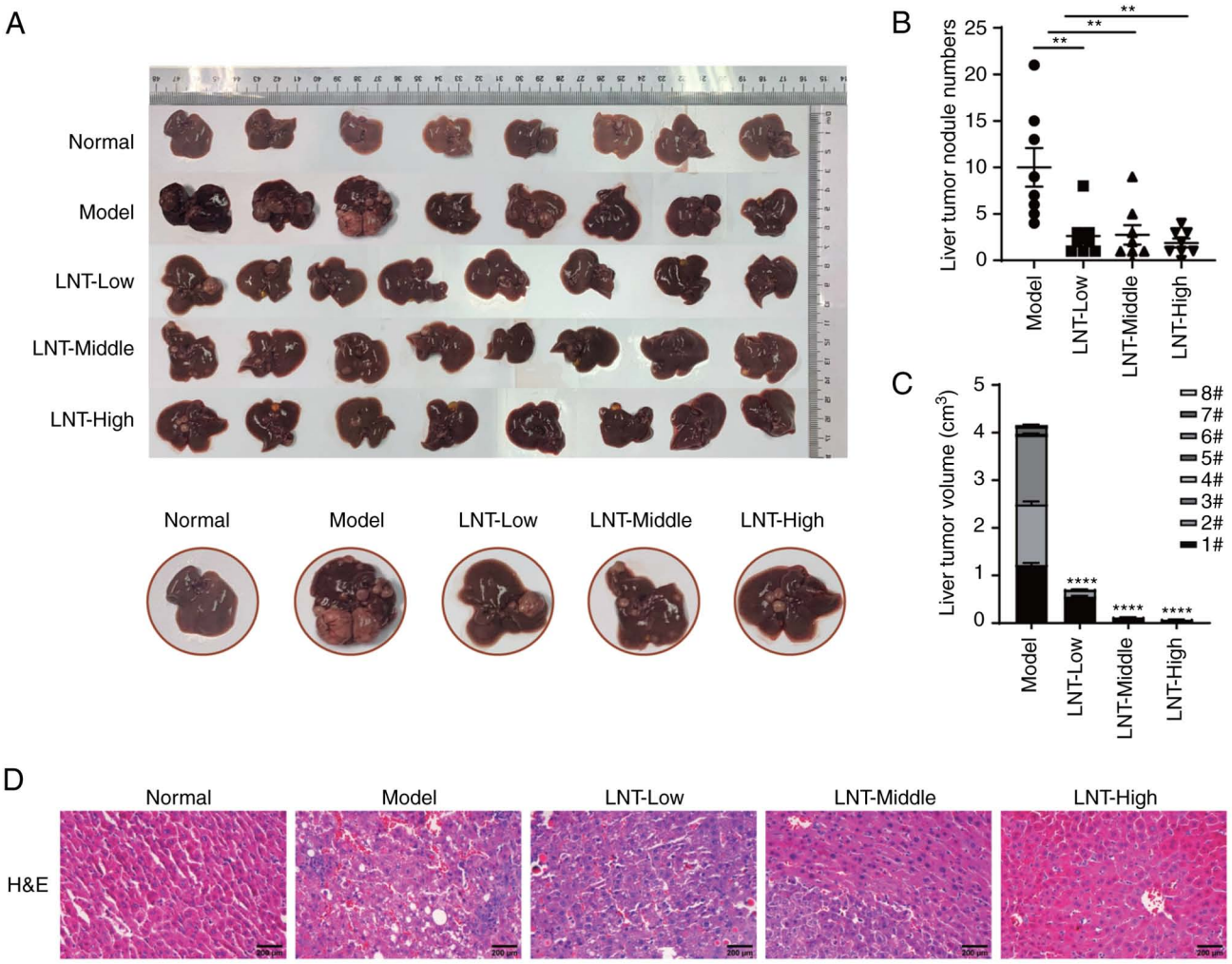

Figure 3. Histopathology of liver tissue from mice with DEN-induced primary liver cancer after LNT treatment. (A) Histopathology of mouse liver tissues. (B) The number of hyperplastic nodules of mice liver tissue. (C) The volume of mice liver tumor nodules. (D) H&E staining of liver tissue sections from mice. Magnification, x400. Scale bars, 200 μm (black). **P<0.01 and ****P<0.0001. DEN, diethylnitrosamine; LNT, Lentinan; H&E, hematoxylin-eosin.

In the present study, it was found that LNT could restore the expression of EGR1 in mouse HCC cells. EGR1 belongs to the Cys2His2-type family of zinc finger proteins and is encoded by the human *EGR1* gene (43). It is a nuclear protein with a transcriptional function (17). At present, the role of EGR1 in liver disease remains controversial. Various studies have suggested that EGR1 can accelerate the development of liver injury (44-46). However, Pritchard *et al* (47,48) in two separate occasions reported that EGR1 can upregulate the expression of hepatoprotective factors and attenuate carbon tetrachloride-induced liver injury. The results of these two studies are diametrically opposed. A recent study (49) found that whilst EGR1 expression is upregulated during the initial stages of liver injury, silencing EGR1 expression aggravated acetaminophen-induced liver injury (AILI). By contrast, overexpression of EGR1 attenuated AILI. It has been hypothesized that the expression of EGR1 in liver tissues can vary across different stages of liver injury. During the early stages of liver injury, the upregulation of EGR1 expression appears to be a protective mechanism. However, in the stage of liver cancer, the expression of EGR1 in HCC cells is suppressed and exhibits low levels of expression compared with normal liver tissue. This is consistent with the *in vivo* data in the present study, where EGR1 expression in the model group was lower than in the normal group. However, after LNT treatment, it not only promoted the expression of EGR1 in mouse HCC cell but also found that LNT could regulate EGR1 into the nucleus and play a transcriptional role *in vitro* nuclear-separation experiments, cell immunofluorescence experiments and *in vivo* IHC experiments.

Subsequently, the present study also showed that PTEN serves an important role in the LNT-induced regulation of EGR1 expression and induction of apoptosis. The *PTEN* gene is a tumor suppressor with dual-specific phosphatase activity (50). Numerous studies have found that the expression of PTEN protein is closely associated with primary liver cancer (51-55). PTEN has been reported to be mutated, inactivated and decreasingly expressed in numerous malignant tumors (56), which need to be supplemented by re-synthesis. In the present study, as the dosage of LNT treatment increased, PTEN expression also increased. In addition, PTEN expression was significantly increased in cells overexpressing EGR1. Therefore, the changes in PTEN expression are likely to be caused by the upregulation of EGR1 by LNT since PTEN is

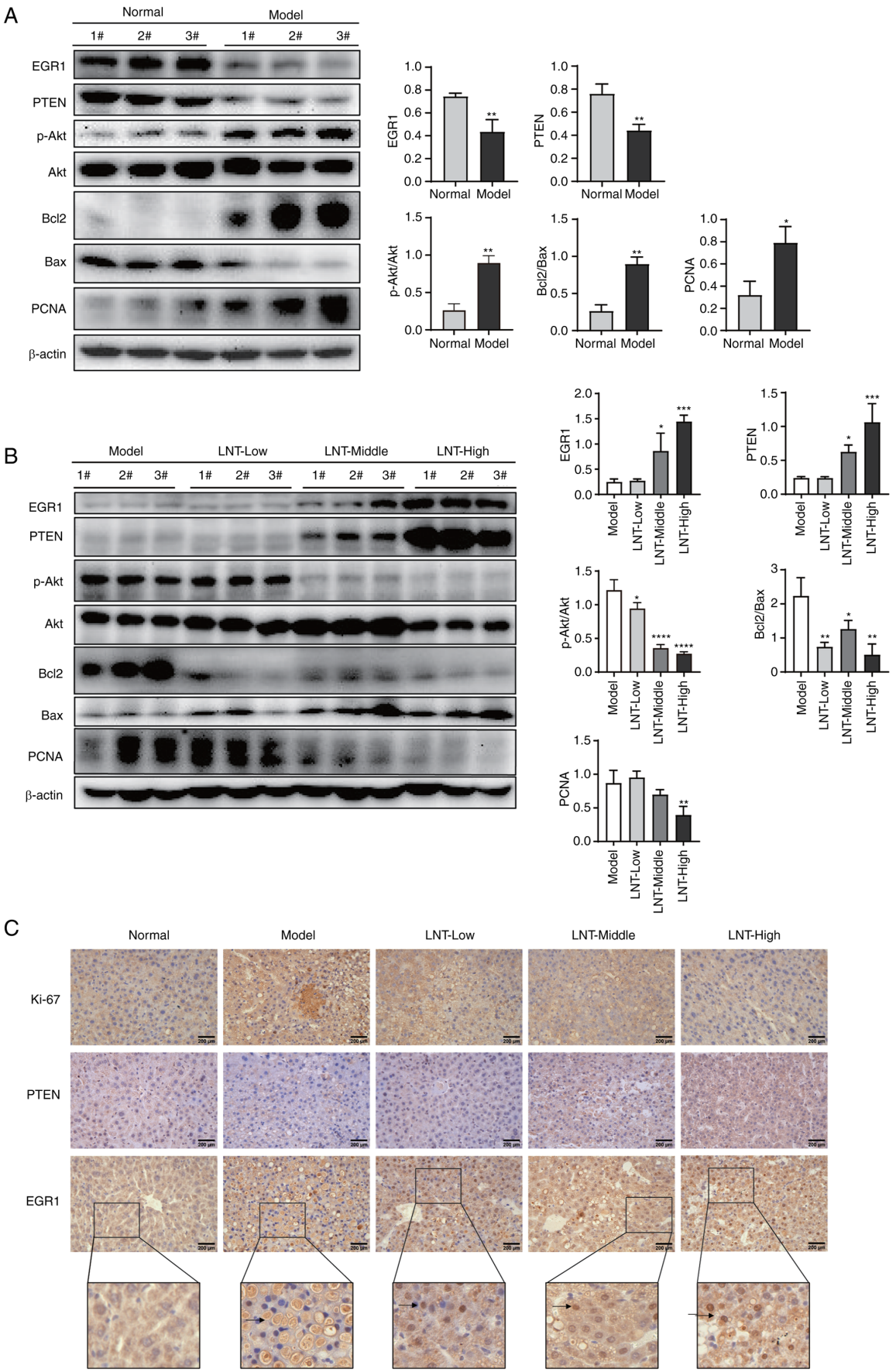

Figure 4. Inhibitory effect of LNT on DEN-induced primary liver cancer in mice. (A) The expression levels of EGR1, PTEN and other proteins in the liver tissues of the normal group and the model group, as analyzed by WB. (B) Expression of EGR1, PTEN and other proteins in liver tissues of the model and LNT-treated groups, as analyzed by WB. (C) Immunohistochemical analysis of EGR1, PTEN and Ki-67 in the tissue sections. Magnification, x400. Scale bars, 200 μm (black). *P<0.05, **P<0.01, ***P<0.001 and ****P<0.0001. LNT, Lentinan; DEN, diethylnitrosamine; EGR1, early growth response 1; WB, western blotting; p-, phosphorylated; PCNA, proliferating cell nuclear antigen.

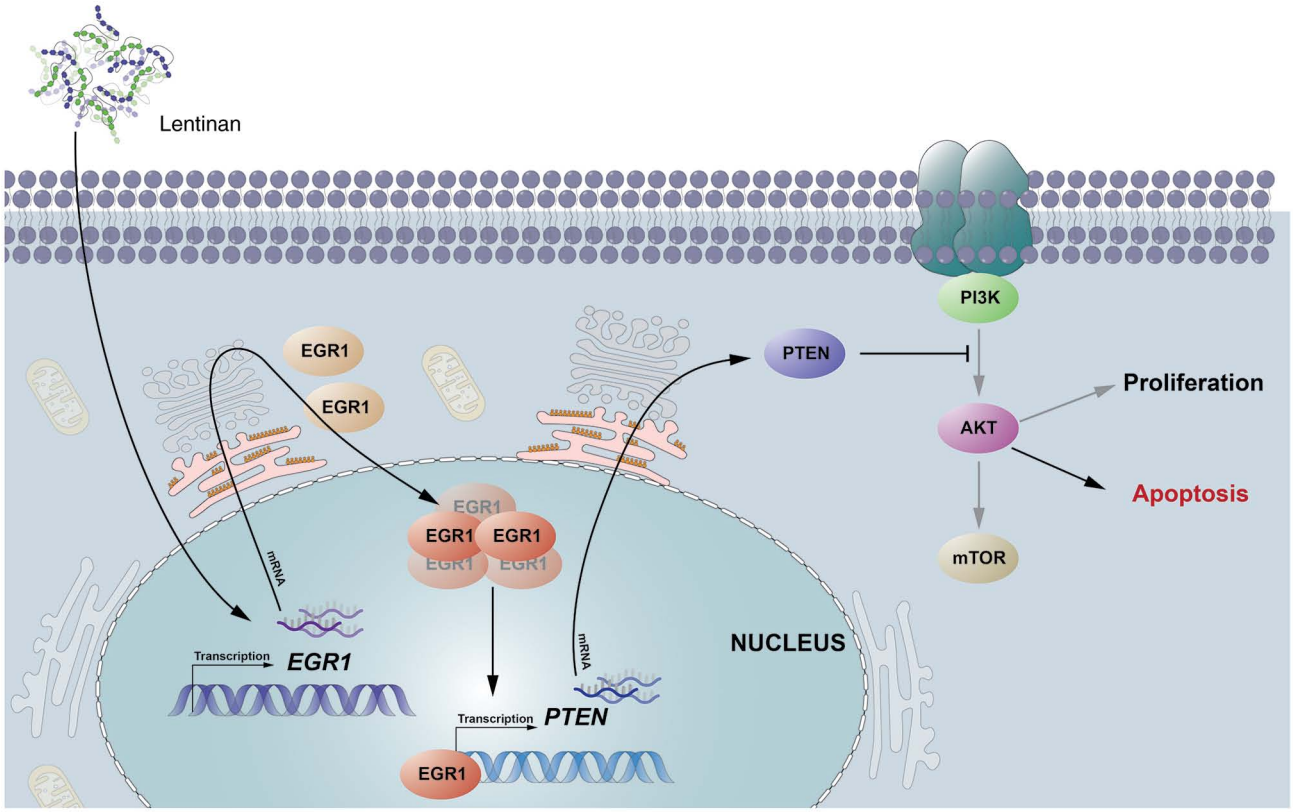

Figure 5. Possible mechanism of LNT against liver cancer through the EGR1/PTEN/AKT axis. Blunt arrows indicate that the signaling pathways are inhibited, whilst pointed arrows indicate that the signaling pathways are activated. LNT, Lentinan; EGR1, early growth response 1.

considered as the direct downstream target of EGR1. Similar results have been reported in papillary thyroid carcinoma and lung cancer cells (29,30).

PTEN is essential for maintaining the balance of the PI3K/AKT signaling pathway (24-28). Several previous studies have reported that increased expression of PTEN can inhibit AKT phosphorylation; inhibition of the AKT signaling pathway can activate the expression of the pro-apoptotic protein Bax whilst inhibiting the expression of the anti-apoptotic protein Bcl-2, ultimately resulting in the apoptosis of cancer cells (57-60). In the present study, as the LNT concentration increased, the expression of PTEN also increased, whilst the phosphorylation of Akt was significantly decreased. Furthermore, Bcl-2 expression decreased and Bax expression increased. Finally, apoptosis of mouse HCC cells occurred.

However, the present study has several limitations. It is generally considered that Caspase-3 is the most crucial terminal shearing enzyme in cell apoptosis. Unfortunately, Caspase-3 and its cleavage products were not detected in the study of LNT on mouse HCC apoptosis. Moreover, when the TUNEL staining test was performed on the tissue sections of the primary liver cancer mouse model in our previous experiment, an intense staining background was identified, rendering it impossible to evaluate whether apoptosis occurs accurately. The reason may be that liver tissue is rich in endogenous peroxidase, which is easy to stain non-specifically. Therefore, the TUNEL staining result was not included in the results of the present study; this will be explored in future study by the authors.

The results of the present study suggested that LNT could inhibit the progression of mouse HCC by regulating the expression and nuclear translocation of EGR1 in mouse HCC cells, activating the expression of the tumor suppressor PTEN. This inhibited activation of the AKT signaling pathway, promoting the apoptosis of mouse HCC. Therefore, LNT can exert its tumor-inhibitory function by increasing the expression of EGR1 during hepatocarcinogenesis. A possible mechanism by which LNT induces apoptosis and stops the progression of mouse HCC through the EGR1/PTEN/AKT axis is shown in Fig. 5.

In the present study, the effect of LNT on HCC cell line Hepa1-6 and its possible mechanism were investigated *in vitro* and *in vivo*. The results showed that LNT could induce apoptosis of Hepa1-6 cells. In addition, LNT promotes the expression of transcription factor EGR1 and regulates EGR1 into the nucleus to promote the expression of tumor suppressor gene PTEN. PTEN then inhibits activation of the AKT signaling pathway, stimulating the occurrence of apoptosis in HCCs. Therefore, it is suggested that LNT can induce apoptosis and cease the progression of mouse HCC through the EGR1/PTEN/AKT signaling axis. These results lay a foundation for exploring the mechanism of anti-HCC by LNT and provide novel ideas for the treatment of primary liver cancer.

Acknowledgements

The authors are grateful to the members of Pan Laboratory from Minnan Normal University for discussion and technical assistance.

Funding

The present study was supported by the National Science and Technology Planning Project of China (grant no. 2021L3027), the New Agricultural Science Education and Practice Project (Letter No. [2020]/20 from Higher Education Department of Education Ministry), the Natural Science Foundation of China (grant no. 81903665), the Natural Science Foundation of Fujian Province (grant no. 2020J01822), the Fujian Province Foreign Cooperation Project (grant no. 2022I0022) and the Cultivation Project of Minnan Normal University (grant no. MSPY202101).

Availability of data and materials

The datasets used and/or analyzed during the current study are available from the corresponding author on reasonable request.

Authors' contributions

YTP and QCW conceptualized the present study. YTP, QCW and YX developed methodology. JPY and YBL validated the data and conducted investigation. JPY and XML performed formal analysis. XML provided resources. ZCL and JFH curated the data. JPY prepared the original draft. YTP and QCW wrote, reviewed and edited the manuscript. AG and YX performed data visualization. QCW supervised the study. YTP conducted project administration. YTP, QCW, ZCL and YX acquired funding. YTP and QCW confirm the authenticity of all the raw data. All authors have read and approved the final version of the manuscript.

Ethics approval and consent to participate

The present study was approved (approval no. 2020010) and supervised by the Animal Ethics and Welfare Committee of Minnan Normal University (Zhangzhou, China). All animal experiments were performed according to the relevant regulatory standards and were performed in accordance with the Experimental animal research Ethics and Welfare Committee of Minna Normal University.

Patient consent for publication

Not applicable.

Competing interests

The authors declare that they have no competing interests.

References

1. Vannucci L, Krizan J, Sima P, Stakheev D, Caja F, Rajsiglova L, Horak V and Saieh M: Immunostimulatory properties and antitumor activities of glucans (Review). Int J Oncol 43: 357-364, 2013.
2. Schepetkin IA and Quinn MT: Botanical polysaccharides: Macrophage immunomodulation and therapeutic potential. Int Immunopharmacol 6: 317-333, 2006.
3. Wasser SP: Medicinal mushrooms as a source of antitumor and immunomodulating polysaccharides. Appl Microbiol Biotechnol 60: 258-274, 2002.
4. Sheng K, Wang C, Chen B, Kang M, Wang M, Liu K and Wang M: Recent advances in polysaccharides from Lentinus edodes (berk.): Isolation, structures and bioactivities. Food Chem 358: 129883, 2021.
5. Bisen PS, Baghel RK, Sanodiya BS, Thakur GS and Prasad GB: Lentinus edodes: A macrofungus with pharmacological activities. Curr Med Chem 17: 2419-2430, 2010.
6. Li S, Huang Y, Wang S, Xu X and Zhang L: Determination of the triple helical chain conformation of β-glucan by facile and reliable triple-detector size exclusion chromatography. J Phys Chem B 118: 668-675, 2014.
7. Zhang X, Li T, Liu S, Xu Y, Meng M, Li X, Lin Z, Wu Q, Xue Y, Pan Y and Alitongbieke G: β-glucan from Lentinus edodes inhibits breast cancer progression via the nur77/hif-1alpha axis. Biosci Rep 40: BSR20201006, 2020.
8. Zhang Q, Du Z, Zhang Y, Zheng Z, Li Q and Wang K: Apoptosis induction activity of polysaccharide from Lentinus edodes in H22-bearing mice through ROS-mediated mitochondrial pathway and inhibition of tubulin polymerization. Food Nutr Res 64: 4364, 2020.
9. Sun M, Bu R, Zhang B, Cao Y, Liu C and Zhao W: Lentinan inhibits tumor progression by immunomodulation in a mouse model of bladder cancer. Integr Cancer Ther 19: 1-7, 2020.
10. Xu H, Qi Z, Zhao Q, Xue J, Zhu J, He Y, Liu G and Qin S: Lentinan enhances the antitumor effects of Delta-like 1 via neutrophils. BMC Cancer 22: 918, 2022.
11. Sung H, Ferlay J, Siegel RL, Laversanne M, Soerjomataram I, Jemal A and Bray F: Global cancer statistics 2020: Globocan estimates of incidence and mortality worldwide for 36 cancers in 185 countries. CA Cancer J Clin 71: 209-249, 2021.
12. Lin J, Shi J, Guo H, Yang X, Jiang Y, Long J, Bai Y, Wang D, Yang X, Wan X, *et al*: Alterations in DNA damage repair genes in primary liver cancer. Clin Cancer Res 25: 4701-4711, 2019.
13. Gingold JA, Zhu D, Lee DF, Kaseb A and Chen J: Genomic profiling and metabolic homeostasis in primary liver cancers. Trends Mol Med 24: 395-411, 2018.
14. Song J, Zhou H, Gu D and Xu Y: Hepatocellular carcinoma differentiation: Research progress in mechanism and treatment. Front Oncol 11: 790358, 2021.
15. Berger E, Vega N, Vidal H and Geloen A: Gene network analysis leads to functional validation of pathways linked to cancer cell growth and survival. Biotechnol J 7: 1395-1404, 2012.
16. Liu S, Yao X, Zhang D, Sheng J, Wen X, Wang Q, Chen G, Li Z, Du Z and Zhang X: Analysis of transcription factor-related regulatory networks based on bioinformatics analysis and validation in hepatocellular carcinoma. Biomed Res Int 2018: 1431396, 2018.
17. Wang B, Guo H, Yu H, Chen Y, Xu H and Zhao G: The role of the transcription factor Egr1 in cancer. Front Oncol 11: 642547, 2021.
18. Yu J, Zhang SS, Saito K, Williams S, Arimura Y, Ma Y, Ke Y, Baron V, Mercola D, Feng GS, *et al*: Pten regulation by AKT-EGR1-ARF-PTEN axis. EMBO J 28: 21-33, 2009.
19. Cui J and Placzek WJ: Post-transcriptional regulation of anti-apoptotic Bcl2 family members. Int J Mol Sci 19: 308, 2018.
20. Lalier L, Cartron PF, Juin P, Nedelkina S, Manon S, Bechinger B and Vallette FM: Bax activation and mitochondrial insertion during apoptosis. Apoptosis 12: 887-896, 2007.
21. Liu Y, Huang Y, Ding J, Liu N, Peng S, Wang J, Wang F and Zhang Y: Targeting akt by SC66 triggers GSK-3β mediated apoptosis in colon cancer therapy. Cancer Cell Int 19: 124, 2019.
22. Yamaguchi H and Wang HG: The protein kinase PKB/Akt regulates cell survival and apoptosis by inhibiting Bax conformational change. Oncogene 20: 7779-7786, 2001.
23. Chen TA, Wang JL, Hung SW, Chu CL, Cheng YC and Liang SM: Recombinant VP1, an Akt inhibitor, suppresses progression of hepatocellular carcinoma by inducing apoptosis and modulation of CCl2 production. PLoS One 6: e23317, 2011.
24. Hopkins BD, Hodakoski C, Barrows D, Mense SM and Parsons RE: PTEN function: The long and the short of it. Trends Biochem Sci 39: 183-190, 2014.
25. Li C and Li X: Circpten suppresses colorectal cancer progression through regulating PTEN/AKT pathway. Mol Ther Nucleic Acids 26: 1418-1432, 2021.
26. Li R, Xing QW, Wu XL, Zhang L, Tang M, Tang JY, Wang JZ, Han P, Wang SQ, Wang W, *et al*: Di-n-butyl phthalate epigenetically induces reproductive toxicity via the PTEN/AKT pathway. Cell Death Dis 10: 307, 2019.
27. Cui Z, Gao H, Yan N, Dai Y, Wang H, Wang M, Wang J, Zhang D, Sun P, Qi T, *et al*: Lncrna plncrna-1 accelerates the progression of prostate cancer by regulating PTEN/Akt axis. Aging (Albany NY) 13: 12113-12128, 2021.

28. Zhang X, Liu C, Li H and Guo L: Effects of mir-21 on proliferation and apoptosis of wt cells via PTEN/Akt pathway. Exp Ther Med 19: 2155-2160, 2020.
29. Guo H and Zhang L: Egr1/2 inhibits papillary thyroid carcinoma cell growth by suppressing the expression of PTEN and BAX. Biochem Genet 59: 1544-1557, 2021.
30. Yamamoto C, Basaki Y, Kawahara A, Nakashima K, Kage M, Izumi H, Kohno K, Uramoto H, Yasumoto K, Kuwano M and Ono M: Loss of PTEN expression by blocking nuclear translocation of EGR1 in gefitinib-resistant lung cancer cells harboring epidermal growth factor receptor-activating mutations. Cancer Res 70: 8715-8725, 2010.
31. Denisenko TV, Sorokina IV, Gogvadze V and Zhivotovsky B: Mitotic catastrophe and cancer drug resistance: A link that must to be broken. Drug Resist Updat 24: 1-12, 2016.
32. Dutta S, Mahalanobish S, Saha S, Ghosh S and Sil PC: Natural products: An upcoming therapeutic approach to cancer. Food Chem Toxicol 128: 240-255, 2019.
33. Chihara G, Maeda Y, Hamuro J, Sasaki T and Fukuoka F: Inhibition of mouse sarcoma 180 by polysaccharides from lentinus edodes (berk.) sing. Nature 222: 687-688, 1969.
34. Yu Z, Ming G, Kaiping W, Zhixiang C, Liquan D, Jingyu L and Fang Z: Structure, chain conformation and antitumor activity of a novel polysaccharide from lentinus edodes. Fitoterapia 81: 1163-1170, 2010.
35. Zhang Y, Zhang M, Jiang Y, Li X, He Y, Zeng P, Guo Z, Chang Y, Luo H, Liu Y, *et al*: Lentinan as an immunotherapeutic for treating lung cancer: A review of 12 years clinical studies in China. J Cancer Res Clin Oncol 144: 2177-2186, 2018.
36. Chen YW, Hu DJ, Cheong KL, Li J, Xie J, Zhao J and Li SP: Quality evaluation of lentinan injection produced in china. J Pharm Biomed Anal 78-79: 176-182, 2013.
37. Zhang M, Zhang Y, Zhang L and Tian Q: Mushroom polysaccharide lentinan for treating different types of cancers: A review of 12 years clinical studies in China. Prog Mol Biol Transl Sci 163: 297-328, 2019.
38. Murata Y, Shimamura T, Tagami T, Takatsuki F and Hamuro J: The skewing to Th1 induced by lentinan is directed through the distinctive cytokine production by macrophages with elevated intracellular glutathione content. Int Immunopharmacol 2: 673-689, 2002.
39. Maeda YY and Chihara G: Lentinan, a new immuno-accelerator of cell-mediated responses. Nature 229: 634, 1971.
40. Zhang Y, Liu Y, Zhou Y, Zheng Z, Tang W, Song M, Wang J and Wang K: Lentinan inhibited colon cancer growth by inducing endoplasmic reticulum stress-mediated autophagic cell death and apoptosis. Carbohydr Polym 267: 118154, 2021.
41. Ya G: A Lentinus edodes polysaccharide induces mitochondrial-mediated apoptosis in human cervical carcinoma HeLa cells. Int J Biol Macromol 103: 676-682, 2017.
42. Chen Q, Zheng Y, Chen X, Ge P, Wang P and Wu B: Upregulation of miR-216a-5p by lentinan targeted inhibition of JAK2/STAT3 signaling pathway to reduce lung adenocarcinoma cell stemness, promote apoptosis, and slow down the lung adenocarcinoma mechanisms. Front Oncol 11: 778096, 2021.
43. Yang Y, Wu F, Zhang J, Sun R, Li F, Li Y, Chang S, Wang L, Wang X, Liu L and Huang C: Egr1 interacts with DNMT3L to inhibit the transcription of miR-195 and plays an anti-apoptotic role in the development of gastric cancer. J Cell Mol Med 23: 7372-7381, 2019.
44. Bi JG, Zheng JF, Li Q, Bao SY, Yu XF, Xu P and Liao CX: Microrna-181a-5p suppresses cell proliferation by targeting Egr1 and inhibiting Egr1/TGF-β/Smad pathway in hepatocellular carcinoma. Int J Biochem Cell Biol 106: 107-116, 2019.
45. Pritchard MT and Nagy LE: Ethanol-induced liver injury: Potential roles for egr-1. Alcohol Clin Exp Res 29: 146S-150S, 2005.
46. Pritchard MT, Roychowdhury S, McMullen MR, Guo L, Arteel GE and Nagy LE: Early growth response-1 contributes to galactosamine/lipopolysaccharide-induced acute liver injury in mice. Am J Physiol Gastrointest Liver Physiol 293: G1124-G1133, 2007.
47. Pritchard MT, Cohen JI, Roychowdhury S, Pratt BT and Nagy LE: Early growth response-1 attenuates liver injury and promotes hepatoprotection after carbon tetrachloride exposure in mice. J Hepatol 53: 655-662, 2010.
48. Pritchard MT, Malinak RN and Nagy LE: Early growth response (EGR)-1 is required for timely cell-cycle entry and progression in hepatocytes after acute carbon tetrachloride exposure in mice. Am J Physiol Gastrointest Liver Physiol 300: G1124-G1131, 2011.
49. Lei X, Xu Q, Li C, Niu B, Ming Y, Li J, Tang Y, Li X, Tang J, Wu J, *et al*: Egr1 confers protection against acetaminophen-induced hepatotoxicity via transcriptional upregulating of Acaa2. Int J Biol Sci 18: 3800-3817, 2022.
50. Worby CA and Dixon JE: PTEN. Annu Rev Biochem 83: 641-669, 2014.
51. Fu X, Wen H, Jing L, Yang Y, Wang W, Liang X, Nan K, Yao Y and Tian T: Microrna-155-5p promotes hepatocellular carcinoma progression by suppressing PTEN through the PI3K/Akt pathway. Cancer Sci 108: 620-631, 2017.
52. Tan L, Xu Z, Mao Q, Zhou S, Zhu J, Zhang X and Li H: Purified PTEN-long induces liver cancer cells to undergo autophagy and apoptosis. Front Surg 9: 767611, 2022.
53. Wang B, Song K, Chen L, Su H, Gao L, Liu J and Huang A: Targeted inhibition of ACK1 can inhibit the proliferation of hepatocellular carcinoma cells through the PTEN/AKT/mTOR pathway. Cell Biochem Funct 38: 642-650, 2020.
54. Xin X, Wu M, Meng Q, Wang C, Lu Y, Yang Y, Li X, Zheng Q, Pu H, Gui X, *et al*: Long noncoding RNA HULC accelerates liver cancer by inhibiting PTEN via autophagy cooperation to miR15a. Mol Cancer 17: 94, 2018.
55. Zhang R, Zhong L, Sun K, Liu J, Wang Q, Mao D, Fang G and Long F: A study on curcumol influencing proliferation and apoptosis of hepatocellular carcinoma cells through DJ-1/PTEN/PI3K/AKT pathway. Biomed Res Int 2022: 9912776, 2022.
56. Sulis ML and Parsons R: PTEN: From pathology to biology. Trends Cell Biol 13: 478-483, 2003.
57. Pilling AB and Hwang C: Targeting prosurvival BCL2 signaling through Akt blockade sensitizes castration-resistant prostate cancer cells to enzalutamide. Prostate 79: 1347-1359, 2019.
58. Cui Y, Su Y, Deng L and Wang W: Ginsenoside-rg5 inhibits retinoblastoma proliferation and induces apoptosis through suppressing BCL2 expression. Chemotherapy 63: 293-300, 2018.
59. Zhang L, Ge C, Zhao F, Zhang Y, Wang X, Yao M and Li J: Nrbp2 overexpression increases the chemosensitivity of hepatocellular carcinoma cells via Akt signaling. Cancer Res 76: 7059-7071, 2016.
60. Belkhiri A, Dar AA, Zaika A, Kelley M and El-Rifai W: T-darpp promotes cancer cell survival by up-regulation of BCL2 through Akt-dependent mechanism. Cancer Res 68: 395-403, 2008.